Distribution and carbon isotopic composition of diploptene from epiphytic bryophytes in Wuhan, central China

Jingjing Li [a,1,*], Jiantao Xue [b,1], B. David A. Naafs [c], Yang Yang [d], Yang Huan [d], Deng Liu [e]

[a] *State Key Laboratory of Lake Sciences and Environment, Nanjing Institute of Geography and Limnology, Chinese Academy of Sciences, Nanjing 210008, China*

[b] *Research Center for Environmental Ecology and Engineering, School of Environmental Ecology and Biological Engineering, Wuhan Institute of Technology, Wuhan 430205, China*

[c] *Organic Geochemistry Unit, School of Chemistry, and School of Earth Sciences, Cabot Institute for the Environment, University of Bristol, Bristol BS8 1TS, UK*

[d] *Hubei Key Laboratory of Critical Zone Evolution, School of Geography and Information Engineering, China University of Geosciences, Wuhan, 430078, China*

[e] *School of Environmental Studies, China University of Geosciences, Wuhan 430074, China*

[1] These authors contributed equally to this work: Jingjing Li, Jiantao Xue

* Author for correspondence: jjli@niglas.ac.cn (J. Li)

ABSTRACT

Diploptene is a ubiquitous hopanoid in the geosphere, synthesized by all hopanoid-containing bacteria. Variations in the concentration and stable carbon isotopic composition ($\delta^{13}C$) of diploptene in ancient peats and lignite can be used to reconstruct certain aspects of the wetland methane cycle in the past. However, the sources and mechanisms that control diploptene $\delta^{13}C$ values in wetlands are not fully constrained. To address this, here we determined the distribution and $\delta^{13}C$ values of diploptene, as well as *n*-alkanes, obtained from five genera of epiphytic bryophytes (non-vascular plants such as mosses) that occupy three different habitats: soil, rock, and tree bark. Our data show that the concentrations of diploptene are highly variable with two order of magnitude differences between the various species. Mosses collected from the soil habitat had higher concentrations compared to those from rock and tree habitats. This suggests that the input from some habitats might dominate the sedimentary signal. The $\delta^{13}C$ values of diploptene ($\delta^{13}C_{dip}$) also vary between species with values ranging between –39.2‰ and –31.2‰. Generally, the $\delta^{13}C$ values of diploptene and long chain *n*-alkanes (i.e., C_{29} and C_{31}) are similar (± 2‰) in most of the bryophyte species. This may suggest that diploptene is produced by heterotrophic bacteria that live in symbiosis with the mosses. However, for some bryophytes the $\delta^{13}C_{dip}$ values are much more ^{13}C depleted (> –2‰) compared to long chain *n*-alkanes, implying that for some mosses bacterial methanotrophs or methylotrophs may contribute to the diploptene pool. Our findings expand our understanding of the

biological sources of diploptene in terrestrial epiphytic bryophytes, which will allow for a more detailed interpretation of the long chain *n*-alkanes and diploptene ($\delta^{13}C$ values) in past environmental and paleoclimatic reconstructions.

Keywords: Epiphytic bryophyte, Diploptene, Long chain *n*-alkanes, Carbon isotopic composition

1. Introduction

Diploptene (hop-22(29)-ene) is one of the most common hopanoids and is often present in immature sediments, such as soils, peat deposits, microbial mats, and marine and lacustrine sediments (Venkatesan, 1988; Ries-Kautt and Albrecht, 1989; Prahl et al., 1992; Pancost et al., 2000; Elvert et al., 2001; van Winden et al., 2012; Davies et al., 2016). It is derived from a wide variety of microbial sources, including cyanobacteria, purple non-sulfur bacteria, anammox and nitrifying bacteria, as well as methylotrophic and methanotrophic bacteria (Rohmer et al., 1984; Douka et al., 2001; Sinninghe Damsté et al., 2004; Härtner et al., 2005; Belin et al., 2018; van Winden et al., 2020; Elling et al., 2022). Given the ubiquity of diploptene in bacteria, including in hetero- and methanotrophic bacteria, its stable carbon isotopic composition ($\delta^{13}C$) has been used to reconstruct past dynamics of the carbon cycle (Spooner et al., 1994; Schouten et al., 2001; Lattaud et al., 2021). For example, diploptene is considered to predominantly derive from methanotrophs when its $\delta^{13}C$ value reaches below –60‰

66 due to the uptake of isotopically light, methane-derived, carbon (Pancost et al., 2000;
67 Elvert et al., 2001; Thiel et al., 2001; Davies et al., 2016; Lattaud et al., 2021).
68 However, in many environments methanotrophs are not the only biological source for
69 diploptene (van Winden et al., 2012). The $\delta^{13}C$ values of diploptene ($\delta^{13}C_{dip}$) in peats
70 and modern peat mosses range from ca. –50‰ to –30‰ (Huang et al., 2010; van
71 Winden et al., 2010; Zheng et al., 2014; Inglis et al., 2019), exhibiting only limited
72 ^{13}C depletion as a result of their mixed heterotrophic and methanotrophic origin.
73 Furthermore, methanotrophs that use the serine cycle (type II, alphaproteobacteria)
74 can be important methanotrophs in peat bogs (Chen et al., 2008; Kip et al., 2010),
75 which could use methane and CO_2 as carbon source, diluting the ^{13}C depleted
76 methane-derived signal in diploptene (van Winden et al., 2012). Although in a
77 mesocosm experiment that used ^{13}C-labelled methane to track in situ methanotrophic
78 activity in *Sphagnum* the $\delta^{13}C$ values of diploptene (–41‰ to –34‰) in *Sphagnum*
79 moss were strongly correlated with the incubation temperature and rate of methane
80 production (van Winden et al., 2020), it is still difficult to explicitly distinguish the
81 contribution of ^{13}C-labelled methanotroph-derived diploptene to the total bacterial
82 diploptene pool.
83 Compared to the extensive investigation of diploptene ($\delta^{13}C$) in a global
84 distribution of peat mosses and peat deposits (Inglis et al., 2019; Naafs et al., 2019),
85 the distribution of diploptene in terrestrial epiphytic bryophytes remains largely
86 undetermined (Smith, 1982; Tuba et al., 2011). These mosses that grow on trees,
87 rocks, and soils are the dominant cover plants in many forest ecosystems (Holland-

Moritz et al., 2021), and hence could be a significant source of diploptene to the terrestrial sedimentary hopanoid pool. Although previous work has examined the occurrence of diploptene from an epiphytic bryophyte in Japan (Toyota et al., 1998), our knowledge about the distribution of diploptene and its $\delta^{13}C$ values in epiphytic bryophytes remains limited. Here we investigate the distribution and $\delta^{13}C$ values of diploptene, as well as the long chain *n*-alkanes, in several facultative epiphytic bryophytes collected from three different substrates (i.e., soil, tree bark and rock), to explore the mechanisms that control their abundance and stable carbon isotopic composition.

2. Materials and Methods

2.1. Site description and sample collection

Due to the diverse microclimate and substrata in Wuhan, the capital city of Hubei Province, central China, there is a large variety of epiphytic bryophytes in urban and suburban areas. *Haplocladium* and *Entodonaceae* are the two most abundant moss genera (Liu et al., 2001; Fan et al., 2017). The regional climate of Wuhan is dominated by a typical subtropical East Asian monsoon, with maximum precipitation and temperature in summer when the East Asian summer monsoon prevails, while the intensified East Asian winter monsoon leads to dry and cold weather during the winter (Chen et al., 2019). The mean annual precipitation of this region is ca. 1266 mm, and the mean annual air temperature (MAAT) is 16 °C (Qian et al., 2019).

A total of 14 epiphytic bryophytes from five genera and eight species were obtained, including *Funaria hygrometrica* (n = 3), *Haplocladium angustifolium* (n = 4), *Haplocladium disclor* (n = 1), *Haplocladium strictulum* (n = 1), *Entodon auutrifolius* (n = 1), *Entodon viridulus* (n = 1), *Plagiomnium cuspidatum* (n = 1) and *Taxiphyllum taxirameum* (n = 2) (for more information, see Table 1). Their habitats can be classified into three categories: surface soil (n = 6), rock (n = 6) and tree bark (n = 2) (Table 1).

2.2. Lipid extraction, quantification and stable carbon isotope analysis

Lipid extraction of mosses followed Huang et al. (2010). Briefly, the whole plant was first rinsed thoroughly with distilled water to remove external contaminants, then freeze-dried. About 1 g of each sample was ultrasonically extracted four times with a mixture of dichloromethane (DCM) and methanol (MeOH) (9:1, v/v) for 10 min. An internal standard (cholane, $C_{24}H_{42}$, Sigma-Aldrich) was added prior to extraction. The total lipid extracts were separated into apolar and polar fractions using activated silica gel column chromatography with *n*-hexane and MeOH as the eluting solvents, respectively. The *n*-alkanes and diploptene in the apolar fraction were quantified using a Shimadzu 2010 gas chromatograph with flame ionization detector (GC-FID) equipped with a DB-5 capillary column and identified by gas chromatography–mass spectrometry (GC–MS) equipped with an Agilent 5973A mass selective detector.

The identification of diploptene was based on the comparison of previously published mass spectra (Härtner et al., 2005; Huang et al., 2010; Sessions et al.,

2013). The concentration of each compound was determined by comparative analysis of its peak area with the internal standard (cholane) based on the GC-FID analysis.

The carbon isotopic compositions of *n*-alkanes and diploptene were determined using a Finnigan Trace GC instrument coupled to a Thermo Finnigan Delta Plus XP isotope ratio mass spectrometer. To check the reproducibility, an *n*-alkane standard mixture (C_{16}–C_{30}, Indiana University) with known carbon isotopic composition values was measured between every two samples (Xue et al., 2016). Squalene of known carbon isotopic composition (−19.8‰) was used as an internal standard. The standard deviation for the $\delta^{13}C$ values of standards was < 0.5‰. The stable carbon isotope ratios ($\delta^{13}C$) are reported as per mil (‰) deviations from the Vienna Pee Dee Belemnite (VPDB) standard, calculated using: $\delta^{13}C$ (‰) = $(R_{sample}/R_{standard}) - 1$, where R is the ratio of $^{13}C/^{12}C$ in the sample and standard. The reproducibility (standard deviation) of the $\delta^{13}C$ values for odd numbered long-chain *n*-alkanes and diploptene was better than 0.5‰ based on the replicate analysis of several samples.

3. Results and discussion

3.1. Distribution of n-alkanes and diploptene in epiphytic bryophytes

Three representative chromatograms of the aliphatic fraction are shown in Fig. 1, i.e., *H. angustitolium* collected from the rock habitat (ID: 4, 5 and 6). The *n*-alkane distribution displays a strong odd/even predominance with a dominance of long chain *n*-alkanes (C_{23}–C_{33}), and hence high carbon preference index (CPI) (Table 1, Fig. 2).

154 The summed concentration of long-chain *n*-alkanes (C_{23}–C_{33}) ranged from 5 to 130
155 μg/g dry weight, with an average of ~ 25 μg/g dry weight (Table 1). We assigned
156 mosses to different categories based on the phylogenetic domain and growth habitat:
157 five genera (Fig. 2b–f) and three habitats (Fig. 2g–i). The predominant long chain
158 odd-carbon-numbered *n*-alkanes (C_{27}–C_{31}) of the mosses is consistent with the *n*-
159 alkane distributions found in terrestrial vascular plants (Bush and McInerney, 2013;
160 Diefendorf and Freimuth, 2017), with the long chain odd-carbon-numbered *n*-alkanes
161 as the most abundant homologues. However, the distribution is not uniform across the
162 habitats and genera. For example, *n*-C_{27} is the most abundant homologue in genus
163 *Entodon*, *n*-C_{31} dominates in the genera of *Funaria* and *Taxiphyllum*, while in the
164 genera of *Haplocladium* and *Plagiomnium* *n*-C_{29} dominates (Table 1, Fig. 2b–f). A
165 dominance of the C_{27} to C_{31} *n*-alkanes is consistent with the findings from the moss
166 species (e.g., *Hypnum revolutum*, *Polytrichum commune*, and *Aulacomnium palustre*)
167 collected from peatlands and mires in UK, China and northern Spain (Nott et al.,
168 2000; Huang et al., 2010; Ortiz et al., 2016). However, this distribution is different
169 from that reported for *Sphagnum*, the most abundant moss in acidic peat deposits,
170 where the *n*-alkane distribution is typically dominated by the mid-chain *n*-C_{23} alkane
171 (Baas et al., 2000; Bingham et al., 2010).

172 Diploptene is present in all moss species. Its concentration is highly variable,
173 ranging from 1 to 109 μg/g dry wt, with an average of ~ 20 μg/g dry wt (Table 1, Fig.
174 3). Interestingly, in some mosses, the concentration of diploptene is higher than that
175 found in *Sphagnum* (Huang et al., 2010), indicating that bacteria living with these

176 mosses could also be an important source to the sedimentary pool. Specifically, the
177 sample from *T. taxirameum* collected from soil surfaces (ID: 14; Table 1) has the
178 highest abundance of diploptene with concentrations more than two orders of
179 magnitude higher than those found in *H. disclor* and *F. hygrometrica,* collected from
180 the rocky habitat (ID: 8 and 2; Table 1, Fig. 3). No significant trend between moss
181 species and their concentrations is found (Fig. 3). However, by habitat level, mosses
182 collected from the soil habitat generally have higher concentrations of diploptene
183 compared to mosses from the rock and tree habitats (Table 1). Furthermore, we also
184 noticed varying relationships between the concentrations of diploptene and *n*-alkanes
185 among the moss species. For example, only *T. taxirameum* collected from rock habitat
186 (ID: 14; Fig. 3) has roughly equal amounts of diploptene and *n*-alkanes. The
187 abundance of diploptene is higher than the summed *n*-alkanes in *H. angustitolium*
188 from rock and soil habitats (ID: 4 and 7; Fig. 3), and in *T. taxirameum* from soil
189 habitat (ID: 14; Fig. 3). However, in other moss species, the concentrations of
190 summed *n*-alkanes are considerably higher than diploptene (Fig. 3). These results
191 indicate that the high concentrations of diploptene produced by certain terrestrial
192 epiphytic bryophytes from some habitats could form a major contribution to the
193 hopanoid pool of sedimentary archives.
194
195 *3.2. $\delta^{13}C$ values of n-alkanes and diploptene in epiphytic bryophytes*
196 The stable carbon isotopic compositions of *n*-alkane are reported for the odd *n*-
197 alkanes C_{29} and C_{31} (Table 1; Fig. 2), the concentrations of the other homologues were

too low for compound-specific carbon isotopic analysis. Notably, the average $\delta^{13}C$ values for the *n*-C_{29} (–32.9 ± 1.4‰) was less ^{13}C-depleted compared to *n*-C_{31} (–34.0 ± 1.5‰) (Table 1). The $\delta^{13}C$ values of *n*-C_{29} and *n*-C_{31} fall into the typical range of values previously reported for terrestrial plants and *Sphagnum* mosses (Freimuth et al., 2019; Naafs et al., 2019; Liu and An, 2020). Thus, there is no substantial difference in δ^{13} values for *n*-C_{29} and *n*-C_{31} between terrestrial bryophytes and previously reported values from *Sphagnum*. For example, our data are identical to the average δ^{13} values for *n*-C_{29} and *n*-C_{31} (–32.4‰) reported from a Scottish montane peat bog (Ficken et al., 1998), implying that it is difficult to distinguish moss species using the $\delta^{13}C$ values of long-chain *n*-alkanes only.

The $\delta^{13}C$ values of diploptene have a wider range than the *n*-alkanes, ranging from –39.2‰ to –31.2‰ (Table 1, Fig. 3). The average $\delta^{13}C_{dip}$ value is –34.9‰, which is close to the average value for C_{31} (–34.0‰), but ca. 2‰ more depleted in ^{13}C than the average value of *n*-C_{29} (–32.9‰) (Table 1). However, for individual moss species, the $\delta^{13}C_{dip}$ value shows high variability even for the same species collected from the same habitat. For example, $\delta^{13}C_{dip}$ values in *F. hygrometrica* from the soil habitat vary by 8‰ (ID: 1 and 3; Table 1, Fig. 3). The $\delta^{13}C_{dip}$ values of terrestrial bryophytes are much more enriched compared to those found in some marine and lake environments with an active methanotroph community (Pancost et al., 2000; Thiel et al., 2001; Davies et al., 2016; Lattaud et al., 2021). In comparison, our results fall into the range of $\delta^{13}C_{dip}$ reported from peatlands (–50‰ to –30‰) (Zheng et al., 2014; Inglis et al., 2019), as well as peat mosses collected from China (Huang et al., 2010), UK, and

220 Argentina (van Winden et al., 2010).

221 We also evaluated the average $\delta^{13}C_{dip}$ value by habitats. The average $\delta^{13}C_{dip}$ value
222 from the soil habitat is the most depleted (–35.4 ± 2.8‰), followed by those from the
223 rock habitat (–34.7 ± 2.0‰). The average $\delta^{13}C_{dip}$ value of two moss species that
224 belong to the *Entodon* genus collected from the tree habitat is the most enriched (–
225 33.5 ± 0.9‰) (Table 1; Fig. 3). There is no significant difference in $\delta^{13}C_{dip}$ values
226 between the rock and soil habitats, which could be further demonstrated by an
227 independent sample *t*-test ($t = 0.53$; $p = 0.61$). Thus, species type and habitat are not
228 the main factors affecting diploptene $\delta^{13}C$ values.

229

230 *3.3. Potential sources of diploptene in epiphytic bryophytes*

231 The molecular and isotopic composition of *n*-alkanes and diploptene allows us to
232 explore the sources of diploptene in epiphytic bryophytes. Most of the bryophytes
233 have similar $\delta^{13}C$ values for the long-chain *n*-alkanes and diploptene (Table 1; Fig. 4).
234 For instance, *H. angustitolium* collected from the rock habitat (ID: 4; Fig. 3) has a
235 high ratio of diploptene relative to the summed *n*-alkanes and has a similar $\delta^{13}C_{dip}$
236 value (–33.7‰) compared to *n*-C_{29} (–32.1‰) and *n*-C_{31} (–32.6‰) (Table 1). This
237 could mean that the heterotrophic bacteria that live in symbioses with mosses
238 consume organic substrates like *n*-alkanes. Although direct proof of the interaction
239 between heterotrophs and moss species for our study is lacking, the presence of
240 *Rhizobium*, a heterotrophic N_2 fixer, has been observed in peatland and bryophytes in
241 karst rocky areas (Larmola et al., 2014; Cao et al., 2020).

In contrast, for some samples there is a significant difference between the $\delta^{13}C$ values of long-chain *n*-alkanes and diploptene. For example, *F. hygrometrica* collected from the soil habitat (ID: 1) has the most depleted $\delta^{13}C_{dip}$ value (–39.2‰) among the mosses (Table 1; Fig. 3). The $\delta^{13}C$ value of *n*-alkanes (avg. –33.8‰ for *n*-C_{29}~C_{31}) is clearly more enriched than the $\delta^{13}C_{dip}$ value of this bryophyte (Table 1; Fig. 4). Such ^{13}C-depleted values could imply that diploptene may partly derive from endophytic methanotrophic bacteria that are in symbiosis with these mosses. This can be confirmed by the presence of *Methylobacterium* on the surface of *F. hygrometrica*, a *Funaria*-associated *Methylobacterium* which can utilize methanol emitted by the stomata of plants (Hornschuh et al., 2002). This is in agreement with previous studies that suggested methylotrophs are abundant in peat ecosystems (Chen et al., 2008), and the phyllosphere and rhizosphere of mosses (Hornschuh et al., 2002; Tani et al., 2012; Iguchi et al., 2015).

Interaction between mosses and methanotrophic and methylotrophic bacteria has been observed in peat bogs (Raghoebarsing et al., 2005; Kip et al., 2010) and karst rocky desertification areas (Cao et al., 2020). On the other hand, *T. taxirameum* which was collected from the soil habitat (ID: 14) has the highest amount of diploptene among the mosses (Fig. 3) and has a more enriched $\delta^{13}C$ value for the *n*-alkanes (avg. –34.7‰ for *n*-C_{29}~C_{31}) compared to $\delta^{13}C_{dip}$ (–37.4‰) (Table 1 and Fig. 4).

In general, the difference between average values of long chain *n*-alkanes (*n*-C_{29}~C_{31}) and diploptene ($\Delta^{13}C_{alk\text{-}dip}$) is < 2‰ in most of the mosses (Fig. 4). This could indicate that diploptene is derived from heterotrophic bacteria, which utilized a

variety of substrates such as *n*-alkanes. In contrast, mosses with a large $\Delta^{13}C_{alk\text{-}dip}$ offset likely have a contribution from bacterial methanotrophs and methylotrophs (Kip et al., 2010). Overall, our results demonstrate that methylotrophic and heterotrophic bacteria are both present in these mosses. Mosses emit methane and methanol (C1 compounds) from their phyllosphere and provide habitats for methylotrophs and heterotrophs. Meanwhile, methanotrophs/methylotrophs convert methane/methanol into organic compounds, which are further utilized by heterotrophs. Thus, our data are indicative of a mutually beneficial interactions between mosses and methylotrophic and heterotrophic bacteria.

We also measured the $\Delta^{13}C_{alk\text{-}dip}$ values by species and habitat, however no significant differences were observed (Fig. 4). Previous studies of diploptene in terrestrial environments have mainly been focused on the *Sphagnum* moss-associated methanotrophs in peatland (van Winden et al., 2020) where methanotrophic activity is evident. Methane concentrations would be relatively low in the environments where we obtained our terrestrial bryophytes, consistent with the lack of significantly depleted $\delta^{13}C$ values in most samples.

4. Conclusions

We determined the distribution pattern of diploptene and long chain *n*-alkanes as well as their $\delta^{13}C$ values in epiphytic bryophytes obtained from three different habitats. The concentrations of diploptene and *n*-alkanes in bryophytes show a high variability across species and habitats. Bryophytes collected from the surface of soil

habitat have higher abundance of diploptene compared to those collected from the rock and tree habitats. Likewise, the $\delta^{13}C_{dip}$ values also show a high variability among the bryophytes. In some bryophytes, diploptene and long-chain *n*-alkanes have similar $\delta^{13}C$ values, which can be attributed to the assimilation by shared carbon source(s), i.e., the heterotrophic bacteria that are symbiotic with the bryophytes. However, there are some bryophytes with much more depleted $\delta^{13}C_{dip}$ values than the long chain *n*-alkanes, which could indicate a contribution of methanotrophs or methylotrophs. Thus far, we have not been able to analyze the isotopic composition of methane and CO_2 in these different microhabitats, which could have further assisted in the interpretation of the results. However, our findings provide evidence for the biological sources of diploptene in terrestrial bryophytes. Our study has helped ascertain the occurrence of diploptene and its potential sources in terrestrial environments, which has improved our understanding of the occurrence and $\delta^{13}C$ of the long chain *n*-alkanes and diploptene in paleoenvironmental and paleoclimatic reconstructions.

Acknowledgements

We would like to thank M. Zheng from China University of Geosciences, Wuhan for sample collecting in the field and moss species identification. This work was funded by the National Natural Science Foundation of China (Grant No. 41977384) and the Natural Science Foundation of Jiangsu Province (Grant No. BK20181508). J. Li acknowledges fundings from the Open Foundation of State Key laboratory of Biogeology and Environmental Geology and Hubei Key Laboratory of Critical Zone

Evolution, China University of Geosciences, Wuhan (GBL21805, CZE2022F01). BDAN acknowledges funding through a Royal Society Tata University Research Fellowship. We also like to thank Dr. John Volkman and two anonymous reviewers for their constructive comments and suggestions, which improved the manuscript.

Associate Editor–**Klaas Nierop**

References

Baas, M., Pancost, R., van Geel, B., Sinninghe Damsté, J.S., 2000. A comparative study of lipids in *Sphagnum* species. Organic Geochemistry 31, 535-541.

Belin, B.J., Busset, N., Giraud, E., Molinaro, A., Silipo, A., Newman, D.K., 2018. Hopanoid lipids: from membranes to plant–bacteria interactions. Nature Reviews Microbiology 16, 304-315.

Bingham, E.M., McClymont, E.L., Väliranta, M., Mauquoy, D., Roberts, Z., Chambers, F.M., Pancost, R.D., Evershed, R.P., 2010. Conservative composition of *n*-alkane biomarkers in *Sphagnum* species: Implications for palaeoclimate reconstruction in ombrotrophic peat bogs. Organic Geochemistry 41, 214-220.

Bush, R.T., McInerney, F.A., 2013. Leaf wax *n*-alkane distributions in and across modern plants: Implications for paleoecology and chemotaxonomy. Geochimica et Cosmochimica Acta 117, 161-179.

Cao, W., Xiong, Y., Zhao, D., Tan, H., Qu, J., 2020. Bryophytes and the symbiotic microorganisms, the pioneers of vegetation restoration in karst rocky desertification areas in southwestern China. Applied Microbiology and Biotechnology 104, 873-891.

Chen, W., Wang, L., Feng, J., Wen, Z., Ma, T., Yang, X., Wang, C., 2019. Recent progress in studies of the variabilities and mechanisms of the East Asian

335 Monsoon in a changing climate. Advances in Atmospheric Sciences 36, 887-
336 901.
337 Chen, Y., Dumont, M.G., McNamara, N.P., Chamberlain, P.M., Bodrossy, L., Stralis-
338 Pavese, N., Murrell, J.C., 2008. Diversity of the active methanotrophic
339 community in acidic peatlands as assessed by mRNA and SIP-PLFA analyses.
340 Environmental Microbiology 10, 446-459.
341 Davies, K.L., Pancost, R.D., Edwards, M.E., Walter Anthony, K.M., Langdon, P.G.,
342 Chaves Torres, L., 2016. Diploptene $\delta^{13}C$ values from contemporary
343 thermokarst lake sediments show complex spatial variation. Biogeosciences 13,
344 2611-2621.
345 Diefendorf, A.F., Freimuth, E.J., 2017. Extracting the most from terrestrial plant-
346 derived *n*-alkyl lipids and their carbon isotopes from the sedimentary record: A
347 review. Organic Geochemistry 103, 1-21.
348 Douka, E., Koukkou, A.-I., Drainas, C., Grosdemange-Billiard, C., Rohmer, M., 2001.
349 Structural diversity of the triterpenic hydrocarbons from the bacterium
350 *Zymomonas mobilis*: the signature of defective squalene cyclization by the
351 squalene/hopene cyclase. FEMS Microbiology Letters 199, 247-251.
352 Elling, F.J., Evans, T.W., Nathan, V., Hemingway, J.D., Kharbush, J.J., Bayer, B.,
353 Spieck, E., Husain, F., Summons, R.E., Pearson, A., 2022. Marine and terrestrial
354 nitrifying bacteria are sources of diverse bacteriohopanepolyols. Geobiology 20,
355 399-420.
356 Elvert, M., Whiticar, M.J., Suess, E., 2001. Diploptene in varved sediments of
357 Saanich Inlet: indicator of increasing bacterial activity under anaerobic
358 conditions during the Holocene. Marine Geology 174, 371-383.
359 Fan, M., Wu, Y.-P., Hu, R.-G., Jiang, Y.-B., 2017. Diversity and distribution of
360 bryophytes and their relationship with environmental factors in Wuhan. Plant
361 Science Journal 35, 825-834 (in Chinese with English abstract).
362 Ficken, K.J., Barber, K.E., Eglinton, G., 1998. Lipid biomarker, $\delta^{13}C$ and plant
363 macrofossil stratigraphy of a Scottish montane peat bog over the last two
364 millennia. Organic Geochemistry 28, 217-237.

365 Freimuth, E.J., Diefendorf, A.F., Lowell, T.V., Wiles, G.C., 2019. Sedimentary *n*-
366 alkanes and *n*-alkanoic acids in a temperate bog are biased toward woody
367 plants. Organic Geochemistry 128, 94-107.
368 Härtner, T., Straub, K.L., Kannenberg, E., 2005. Occurrence of hopanoid lipids in
369 anaerobic *Geobacter* species. FEMS Microbiology Letters 243, 59-64.
370 Holland-Moritz, H., Stuart, J.E.M., Lewis, L.R., Miller, S.N., Mack, M.C., Ponciano,
371 J.M., McDaniel, S.F., Fierer, N., 2021. The bacterial communities of Alaskan
372 mosses and their contributions to N_2-fixation. Microbiome 9, 53.
373 Hornschuh, M., Grotha, R., Kutschera, U., 2002. Epiphytic bacteria associated with
374 the bryophyte *Funaria hygrometrica*: effects of *Methylobacterium* strains on
375 protonema development. Plant Biology 4, 682-687.
376 Huang, X., Wang, C., Xue, J., Meyers, P.A., Zhang, Z., Tan, K., Zhang, Z., Xie, S.,
377 2010. Occurrence of diploptene in moss species from the Dajiuhu Peatland in
378 southern China. Organic Geochemistry 41, 321-324.
379 Iguchi, H., Yurimoto, H., Sakai, Y., 2015. Interactions of methylotrophs with plants
380 and other heterotrophic bacteria. Microorganisms 3, 137-151.
381 Inglis, G.N., Naafs, B.D.A., Zheng, Y., Schellekens, J., Pancost, R.D., 2019. $\delta^{13}C$
382 values of bacterial hopanoids and leaf waxes as tracers for methanotrophy in
383 peatlands. Geochimica et Cosmochimica Acta 260, 244-256.
384 Kip, N., van Winden, J.F., Pan, Y., Bodrossy, L., Reichart, G.-J., Smolders, A.J.P.,
385 Jetten, M.S.M., Sinninghe Damsté, J.S., Op den Camp, H.J.M., 2010. Global
386 prevalence of methane oxidation by symbiotic bacteria in peat-moss
387 ecosystems. Nature Geoscience 3, 617-621.
388 Larmola, T., Leppänen, S.M., Tuittila, E.-S., Aarva, M., Merilä, P., Fritze, H., Tiirola,
389 M., 2014. Methanotrophy induces nitrogen fixation during peatland
390 development. Proceedings of the National Academy of Sciences 111, 734-739.
391 Lattaud, J., De Jonge, C., Pearson, A., Elling, F.J., Eglinton, T.I., 2021. Microbial lipid
392 signatures in Arctic deltaic sediments—Insights into methane cycling and
393 climate variability. Organic Geochemistry 157, 104242.
394 Liu, J., An, Z., 2020. Leaf wax *n*-alkane carbon isotope values vary among major

terrestrial plant groups: Different responses to precipitation amount and temperature, and implications for paleoenvironmental reconstruction. Earth-Science Reviews 202, 103081.

Liu, S.-X., Peng, D., Qin, W., Yu, X.-J., Pan, X.-Y., Liu, S., 2001. Studies on the bryophyta plants resources in Hubei Province—□ The bryophytes flora of Wuhan city. Journal of Central China Normal Unversity (Natural Sciences), 35, 326-329 (in Chinese with English abstract).

Naafs, B.D.A., Inglis, G.N., Blewett, J., McClymont, E.L., Lauretano, V., Xie, S., Evershed, R.P., Pancost, R.D., 2019. The potential of biomarker proxies to trace climate, vegetation, and biogeochemical processes in peat: A review. Global and Planetary Change 179, 57-79.

Nott, C.J., Xie, S., Avsejs, L.A., Maddy, D., Chambers, F.M., Evershed, R.P., 2000. *n*-alkane distributions in ombrotrophic mires as indicators of vegetation change related to climatic variation. Organic Geochemistry 31, 231-235.

Ortiz, J.E., Borrego, Á.G., Gallego, J.L.R., Sánchez-Palencia, Y., Urbanczyk, J., Torres, T., Domingo, L., Estébanez, B., 2016. Biomarkers and inorganic proxies in the paleoenvironmental reconstruction of mires: The importance of landscape in Las Conchas (Asturias, Northern Spain). Organic Geochemistry 95, 41-54.

Pancost, R.D., Sinninghe Damsté, J.S., De Lint, S., van der Maarel, M.J.E.C., Gottschal, J.C., 2000. Biomarker evidence for widespread anaerobic methane oxidation in Mediterranean sediments by a consortium of methanogenic Archaea and Bacteria. Applied and Environmental Microbiology 66, 1126-1132.

Prahl, F.G., Hayes, J.M., Xie, T.M., 1992. Diploptene: An indicator of terrigenous organic carbon in Washington coastal sediments. Limnology and Oceanography 37, 1290-1300.

Qian, S., Yang, H., Dong, C., Wang, Y., Wu, J., Pei, H., Dang, X., Lu, J., Zhao, S., Xie, S., 2019. Rapid response of fossil tetraether lipids in lake sediments to seasonal environmental variables in a shallow lake in central China: Implications for the use of tetraether-based proxies. Organic Geochemistry 128, 108-121.

425 Raghoebarsing, A.A., Smolders, A.J.P., Schmid, M.C., Rijpstra, W.I.C., Wolters-Arts,
426 M., Derksen, J., Jetten, M.S.M., Schouten, S., Sinninghe Damsté, J.S., Lamers,
427 L.P.M., Roelofs, J.G.M., Op den Camp, H.J.M., Strous, M., 2005.
428 Methanotrophic symbionts provide carbon for photosynthesis in peat bogs.
429 Nature 436, 1153-1156.
430 Ries-Kautt, M., Albrecht, P., 1989. Hopane-derived triterpenoids in soils. Chemical
431 Geology 76, 143-151.
432 Rohmer, M., Bouvier-Nave, P., Ourisson, G., 1984. Distribution of hopanoid
433 triterpenes in Prokaryotes. Journal of General Microbiology 130, 1137-1150.
434 Schouten, S., Rijpstra, W.I.C., Kok, M., Hopmans, E.C., Summons, R.E., Volkman,
435 J.K., Sinninghe Damsté, J.S., 2001. Molecular organic tracers of
436 biogeochemical processes in a saline meromictic lake (Ace Lake). Geochimica
437 et Cosmochimica Acta 65, 1629-1640.
438 Sessions, A.L., Zhang, L., Welander, P.V., Doughty, D., Summons, R.E., Newman,
439 D.K., 2013. Identification and quantification of polyfunctionalized hopanoids
440 by high temperature gas chromatography–mass spectrometry. Organic
441 Geochemistry 56, 120-130.
442 Sinninghe Damsté, J.S., Rijpstra, W.I.C., Schouten, S., Fuerst, J.A., Jetten, M.S.M.,
443 Strous, M., 2004. The occurrence of hopanoids in planctomycetes: implications
444 for the sedimentary biomarker record. Organic Geochemistry 35, 561-566.
445 Smith, A.J.E., 1982. Epiphytes and Epiliths, in: Smith, A.J.E. (Ed.), Bryophyte
446 Ecology. Springer Netherlands, Dordrecht, pp. 191-227.
447 Spooner, N., Rieley, G., Collister, J.W., Lander, M., Cranwell, P.A., Maxwell, J.R.,
448 1994. Stable carbon isotopic correlation of individual biolipids in aquatic
449 organisms and a lake bottom sediment. Organic Geochemistry 21, 823-827.
450 Tani, A., Takai, Y., Suzukawa, I., Akita, M., Murase, H., Kimbara, K., 2012. Practical
451 application of methanol-mediated mutualistic symbiosis between
452 *Methylobacterium* species and a roof greening moss, *Racomitrium japonicum*.
453 PLoS One 7, e33800.
454 Thiel, V., Peckmann, J., Richnow, H.H., Luth, U., Reitner, J., Michaelis, W., 2001.

Molecular signals for anaerobic methane oxidation in Black Sea seep carbonates and a microbial mat. Marine Chemistry 73, 97-112.

Toyota, M., Masuda, K., Asakawa, Y., 1998. Triterpenoid constituents of the moss *Floribundaria aurea* subsp. *nipponica*. Phytochemistry 48, 297-299.

Tuba, Z., Slack, N.G., Stark, L.R., 2011. Bryophyte Ecology and Climate Change. Cambridge University Press, Cambridge.

van Winden, J.F., Kip, N., Reichart, G.-J., Jetten, M.S.M., Op den Camp, H.J.M., Sinninghe Damsté, J.S., 2010. Lipids of symbiotic methane-oxidizing bacteria in peat moss studied using stable carbon isotopic labelling. Organic Geochemistry 41, 1040-1044.

van Winden, J.F., Talbot, H.M., De Vleeschouwer, F., Reichart, G.-J., Sinninghe Damsté, J.S., 2012. Variation in methanotroph-related proxies in peat deposits from Misten Bog, Hautes-Fagnes, Belgium. Organic Geochemistry 53, 73-79.

van Winden, J.F., Talbot, H.M., Reichart, G.-J., McNamara, N.P., Benthien, A., Sinninghe Damsté, J.S., 2020. Influence of temperature on the $\delta^{13}C$ values and distribution of methanotroph-related hopanoids in *Sphagnum*-dominated peat bogs. Geobiology 18, 1-11.

Venkatesan, M.I., 1988. Diploptene in Antarctic sediments. Geochimica et Cosmochimica Acta 52, 217-222.

Xue, J., Dang, X., Tang, C., Yang, H., Xiao, G., Meyers, P.A., Huang, X., 2016. Fidelity of plant-wax molecular and carbon isotope ratios in a Holocene paleosol sequence from the Chinese Loess Plateau. Organic Geochemistry 101, 176-183.

Zheng, Y., Singarayer, J.S., Cheng, P., Yu, X., Liu, Z., Valdes, P.J., Pancost, R.D., 2014. Holocene variations in peatland methane cycling associated with the Asian summer monsoon system. Nature Communication 5, 4631.

Figure captions

Fig. 1. The total ion chromatogram (TIC) of aliphatic fraction of *Haplocladium angustitolium* that collected on the surface of rock (Sample ID: 4, 5 and 6) with varying amouns of *n*-alkanes and diploptene.

Fig. 2. Histograms of normalized *n*-alkane distribution in bryophytes showing averaged distribution values with mean standard deviation of each genus (b–f) and habitat (g–i) including *n* samples as indicated, overlain by the average stable carbon isotope ($\delta^{13}C$) data for odd-numbered long-chained *n*-alkane (C_{27}, C_{29}, C_{31} and C_{33}) homologues.

Fig. 3. Concentration of the summed *n*-alkanes (C_{23}–C_{33}) and diploptene, and the $\delta^{13}C$ values of diploptene in 14 moss species belong to five genera that collected from three habitats including soil (S), rock (R) and tree (T).

Fig. 4. Differences between the average $\delta^{13}C$ values of long chain *n*-alkanes (C_{29}, C_{31}) and diploptene ($\Delta^{13}C_{alk\text{-}dip}$) across the moss species (a) and habitats (b). The abbreviation refers to the genus of moss in Table 1 and Fig. 2.

Table 1. Quantification and $\delta^{13}C$ values (‰) of *n*-alkanes and diploptene (Dip) in 14 moss species belong to five genera and collected from three habitats including the surface of soil, rock and tree in Wuhan City, China (The standard deviation of $\delta^{13}C$ values is better than ±0.5‰)

ID	Species	Genus	Habitat	*n*-C_{23}	*n*-C_{25}	*n*-C_{27}	*n*-C_{29}	*n*-C_{31}	*n*-C_{33}	Sum	Dip.	*n*-C_{27}	*n*-C_{29}	*n*-C_{31}	*n*-C_{33}	Dip.
				μg/g dry weight								$\delta^{13}C$ (‰)				
1	*Funaria hygrometrica* Hedw.	*Funaria*	Soil	0.2	0.4	1	5	**8**	1	18	4	-34.1	-33.3	-34.2	-34.8	-39.2
2	*Funaria hygrometrica* Hedw.	*Funaria*	Rock	0.5	0.9	2	4	4	**4**	16	1	-33.5	-33.8	-35.0	-36.0	-34.4
3	*Funaria hygrometrica* Hedw.	*Funaria*	Soil	0.2	0.2	0.4	1	**2**	1	7	2	-30.3	-32.9	-34.1	-34.2	-31.2
4	*Haplocladium angustitolium*	*Haplocladium*	Rock	0.4	0.2	0.7	2	**2**		7	34	-30.1	-30.2	-32.1	-32.6	-33.7
5	*Haplocladium angustitolium*	*Haplocladium*	Rock	0.4	0.5	2	10	**12**	2	28	4	-32.6	-31.5	-32.4	-33.5	-38.5
6	*Haplocladium angustitolium*	*Haplocladium*	Rock	0.5	0.6	2	**4**	4	2	16	1	-31.8	-32.5	-32.9	-31.6	-34.2
7	*Haplocladium angustitolium*	*Haplocladium*	Soil	0.4	2	1	2	**3**		10	43		-31.0	-33.1	-38.4	-35.5
8	*Haplocladium disclor*	*Haplocladium*	Rock	0.3	0.4	1	3	2	**4**	11	1	-35.9	-35.4	-35.5	-36.9	-34.7
9	*Haplocladium strictulum*	*Haplocladium*	Soil	2	2	10	38	**39**	30	130	15	-36.8	-34.1	-34.8	-36.7	-36.1
10	*Entodon auutrifolius*	*Entodon*	Tree	0.2	0.1	1	1	**1**	1	5	2		-33.1	-33.5	-33.1	-32.9
11	*Entodon viridulus*	*Entodon*	Tree	0.5	0.5	**7**	3	3	1	16	3	-38.9	-32.7	-32.9	-32.6	-34.1
12	*Plagiomnium cuspidatum*	*Plagiomnium*	Soil	0.5	1	5	**11**	9	4	34	20		-34.4	-37.2	-38.6	-33.3
13	*Taxiphyllum taxirameum*	*Taxiphyllum*	Rock	0.5	3	7	9	**10**	3	36	40	-33.3	-32.3	-33.1	-32.9	-32.7
14	*Taxiphyllum taxirameum*	*Taxiphyllum*	Soil	0.8	2	4	8	**12**		33	109	-35.8	-33.7	-35.7		-37.4

1 **Fig. 1.**

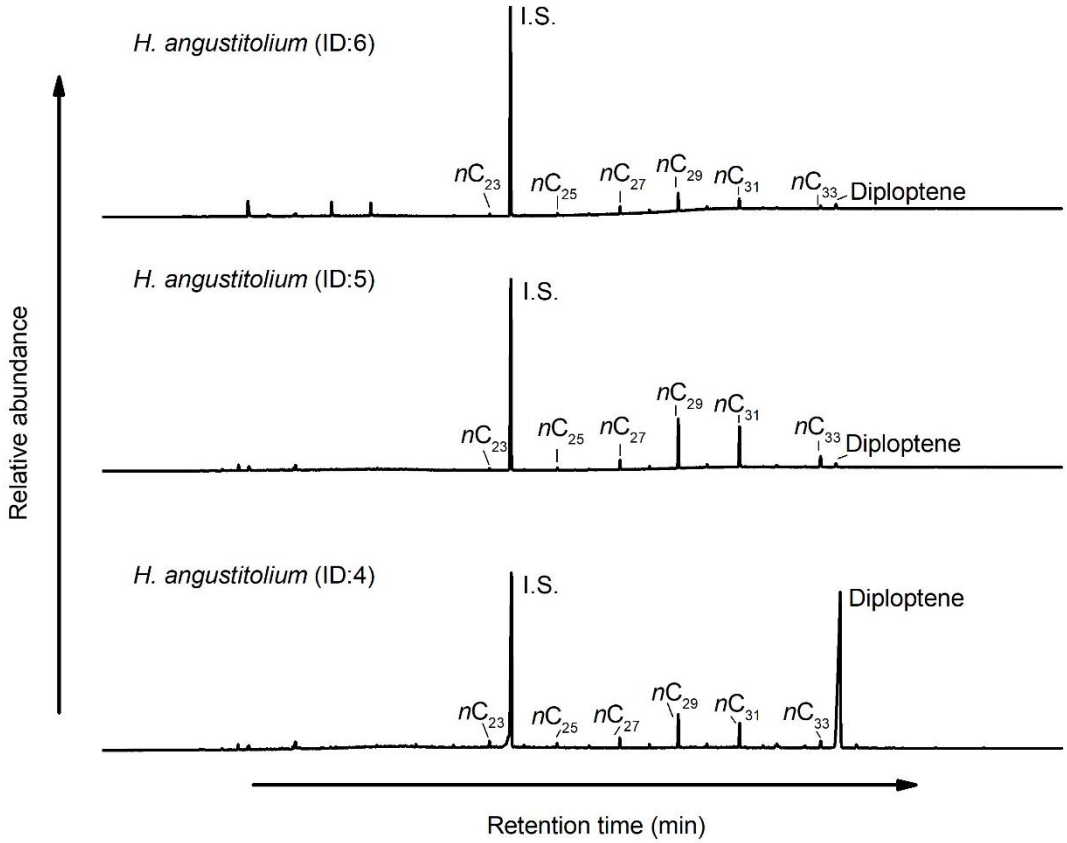

2

3

Fig. 2.

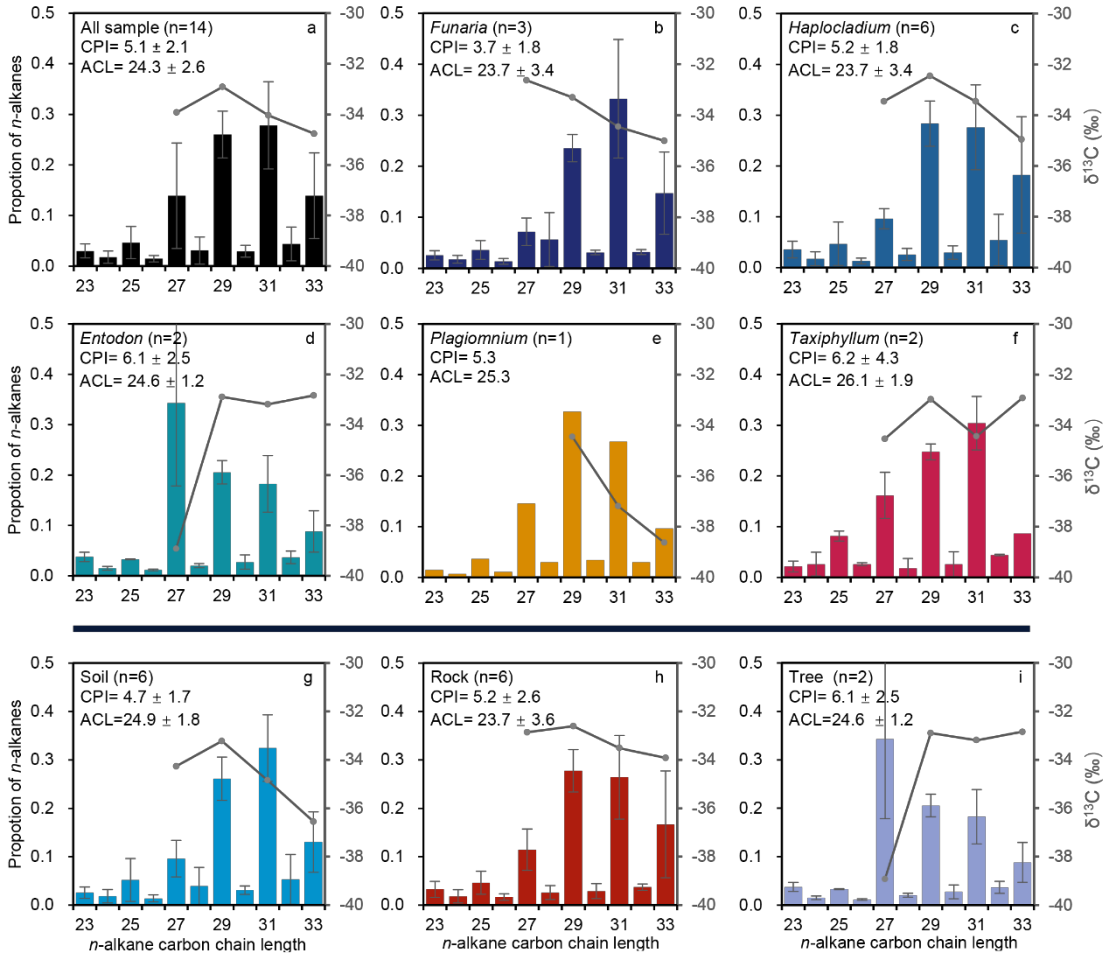
All sample (n=14)
CPI= 5.1 ± 2.1
ACL= 24.3 ± 2.6
a
Funaria (n=3)
CPI= 3.7 ± 1.8
ACL= 23.7 ± 3.4
b
Haplocladium (n=6)
CPI= 5.2 ± 1.8
ACL= 23.7 ± 3.4
c
Entodon (n=2)
CPI= 6.1 ± 2.5
ACL= 24.6 ± 1.2
d
Plagiomnium (n=1)
CPI= 5.3
ACL= 25.3
e
Taxiphyllum (n=2)
CPI= 6.2 ± 4.3
ACL= 26.1 ± 1.9
f
Soil (n=6)
CPI= 4.7 ± 1.7
ACL=24.9 ± 1.8
g
Rock (n=6)
CPI= 5.2 ± 2.6
ACL= 23.7 ± 3.6
h
Tree (n=2)
CPI= 6.1 ± 2.5
ACL=24.6 ± 1.2
i
Propotion of n-alkanes
δ13C (‰)
n-alkane carbon chain length

Fig. 3.

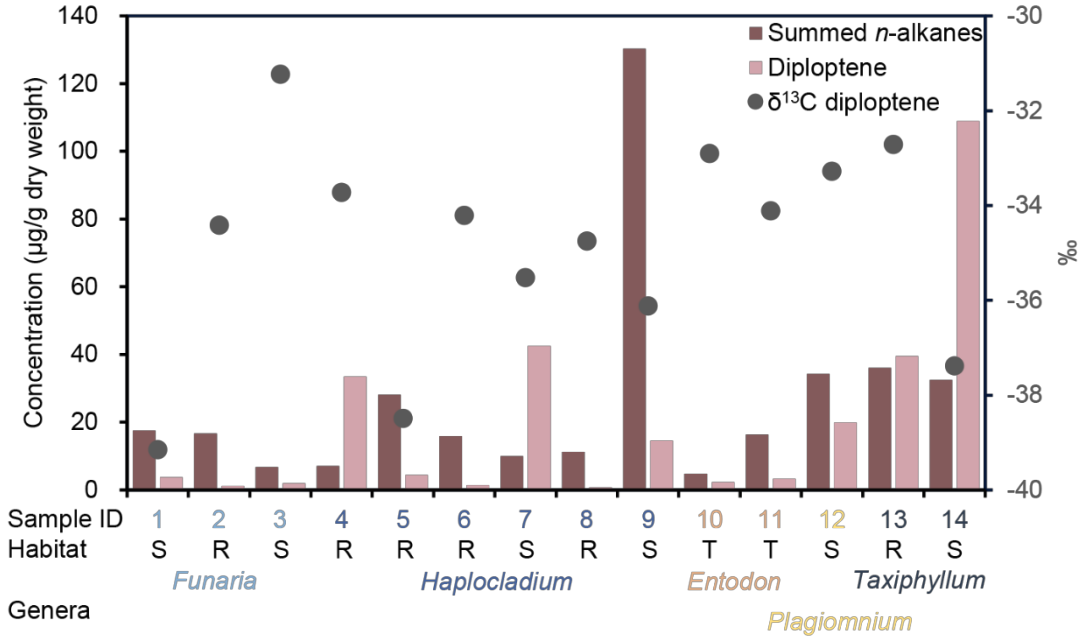
Concentration (µg/g dry weight)
140
120
100
80
60
40
20
0
-30
-32
-34
-36
-38
-40
‰
Summed n-alkanes
Diploptene
δ13C diploptene
Sample ID 1 2 3 4 5 6 7 8 9 10 11 12 13 14
Habitat S R S R R R S R S T T S R S
Genera
Funaria
Haplocladium
Entodon
Taxiphyllum
Plagiomnium

Fig. 4.

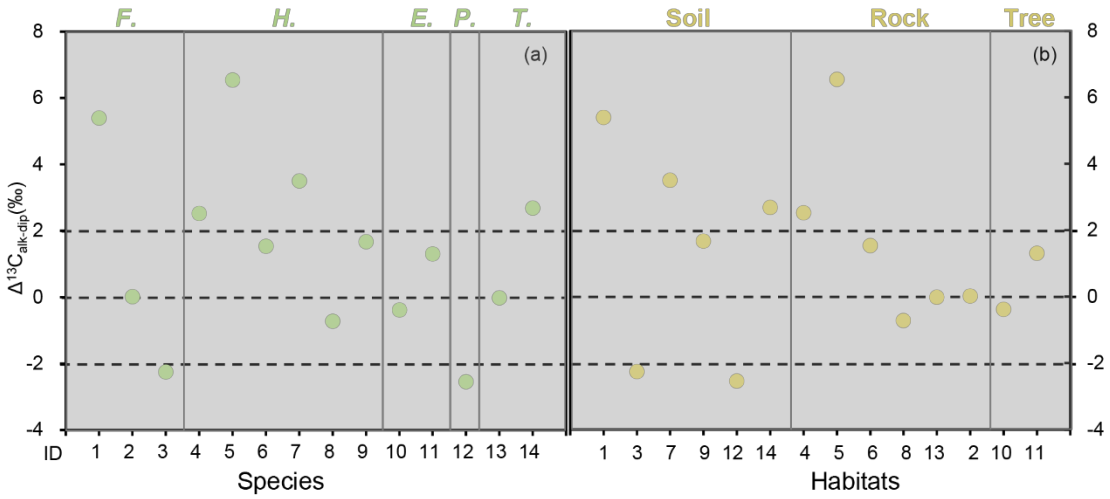
F.
H.
E.
P.
T.
Soil
Rock
Tree
(a)
(b)
8
6
4
2
0
-2
-4
$\Delta^{13}C_{alk\text{-}dip}$ (‰)
ID
1 2 3 4 5 6 7 8 9 10 11 12 13 14
Species
1 3 7 9 12 14 4 5 6 8 13 2 10 11
Habitats